

Geology and mineralization of the AurMac metasediment-hosted gold deposits, central Yukon (NTS 105M/13)

R. Keagan Parry and Pilar Lecumberri-Sanchez*
Earth and Atmospheric Sciences, University of Alberta

Patrick Sack
Yukon Geological Survey

Parry, R.K., Lecumberri-Sanchez, P. and Sack, P., 2025. Geology and mineralization of the AurMac metasediment-hosted gold deposits, central Yukon (NTS 105M/13). In: Yukon Exploration and Geology Technical Papers 2024, L.H. Weston, A. Stuart, S.K. Schultz, A.D. Brubacher and D.C. Cronmiller (eds.), Yukon Geological Survey, p. 19–39.

Abstract

The AurMac property, located 35 km north of Mayo in central Yukon, includes two metasedimentary rock-hosted gold deposits: the 6158 koz Au Powerline deposit and the 845 koz Au Airstrip deposit. Mineralization at the Powerline and Airstrip deposits is characterized by gold in sheeted quartz veins and mineralized skarn horizons, respectively. The AurMac deposits straddle the Robert Service thrust fault whereby the Powerline deposit is hosted in the Late Proterozoic to Cambrian Hyland Group hanging wall, and the Airstrip deposit is hosted in the Mississippian Sourdough Hill Member of the Keno Hill Quartzite footwall. Host rocks comprise siliciclastic metasedimentary rocks, variably calc-silicate-altered calcareous metasedimentary rocks and magmatic rocks. Magmatic rocks in the Powerline zone consist of foliated mafic horizons that are geochemically similar to Cambro-Ordovician magmatic rocks found in Hyland Group metasedimentary rocks in the McQuesten, Mayo, Clark Lakes and Hart River map areas. In the Airstrip zone, magmatic rocks include a steeply south-dipping, unfoliated, aplite dike. Evidence for intrusion-related gold mineralization at AurMac includes sheeted vein and skarn mineralization similar to the intrusion-hosted, intrusion-related gold deposits at Dublin Gulch, as well as the presence of metamorphic porphyroblast assemblages that suggest contact metamorphism. These findings suggest potential for further discovery of mineralized intrusion-hosted zones on the AurMac property and sediment-hosted, intrusion-related gold deposits elsewhere in the region.

Plain language summary

The AurMac project, located 35 km north of Mayo in central Yukon, includes two gold deposits: the Powerline and Airstrip deposits. The Powerline deposit is estimated to contain over six million ounces of gold, and the Airstrip deposit contains nearly one million ounces of gold. Mineralization in the Powerline deposit is found in quartz-rich veins, whereas gold at the Airstrip deposit is found in a type of metamorphic rock known as skarn. The Powerline deposit is hosted in rocks that are approximately 500 million years old, and the Airstrip deposit is hosted in rocks that are approximately 350 million years old. A large fault, known as the Robert Service thrust, separates the two deposits. The mineralization at the AurMac deposits have some similarities to the mineralization that is found in the deposits of the Eagle Gold Mine in central Yukon and suggests the potential for another significant economic deposit of the same style.

* rkparry@ualberta.ca

Introduction

The AurMac property, located in the McQuesten River area of central Yukon (Fig. 1), is situated equidistant between the recently producing Eagle Gold Mine (>5 Moz Au global resource; Harvey et al., 2023) and the currently producing Keno Hill district (>230 Moz Ag global production; Fig. 2; Blais et al., 2024). Two gold deposits have been defined on the property: the Airstrip deposit, containing 845 koz Au at 0.75 g/t Au hosted primarily in skarn horizons, and the Powerline deposit, containing 6158 koz Au at 0.61 g/t Au hosted primarily in sheeted quartz veins (Fig. 3; Thornton et al., 2024). The AurMac deposits are hypothesized to be part of a reduced intrusion-related gold system (RIRGS), similar to the model described for the nearby Dublin Gulch property (e.g., Hart, 2007). However, a key distinction to existing RIRGS models is that rather than gold being hosted within the carapace and surrounding hornfels of an intrusion, gold at AurMac is solely hosted in metasedimentary rocks and a causative intrusion has yet to be identified.

In this contribution, we review an updated and expanded geological context and characterization of mineralization styles of the AurMac deposits based on detailed relogging of drill core, petrography and whole-rock geochemical analyses. A correlation of lithological units observed at the AurMac deposits is made with map units from the nearby Keno Hill district, providing a southwest extension of Keno Hill district map units to the AurMac property. Resolution of the bedrock geology concludes that sheeted quartz vein mineralization observed in the Powerline deposit is hosted in Late Proterozoic to Cambrian Hyland Group metasedimentary rocks, and skarn-hosted mineralization found in the Airstrip deposit is hosted in the Mississippian to Permian(?) Keno Hill Quartzite. Evidence supporting intrusion-related mineralization is also presented, and includes the presence of contact metamorphism-related porphyroblast assemblages and mineralization styles analogous to those found at intrusion-hosted gold deposits.

Regional geology and structural setting

Stratigraphy

The AurMac property is hosted within slope and basinal Laurentian margin strata of the Selwyn basin (Fig. 1), which covers an area approximately 700 by 200 km in central and eastern Yukon. It is characterized by Neoproterozoic to Middle Devonian slope-to-basin

facies strata, related to Neoproterozoic and younger rifting along the North American margin (Gordey and Anderson, 1993; Colpron et al., 2002). The Selwyn basin is bordered by the Mackenzie platform to the north, and the strike-slip Tintina fault to southwest, which mostly separates it from the Yukon-Tanana terrane (Gabrielse et al., 2006). Rocks at the AurMac property consist of Late Proterozoic to Cambrian Hyland Group metasedimentary rocks, and the Mississippian to Permian(?) Keno Hill Quartzite (Murphy, 1997; Read et al., 2020; Figs. 2 and 3).

Foliated mafic rocks within the Hyland Group have been mapped in the northern McQuesten and Mayo map areas (Murphy, 1997). These include fine to medium-grained quartz-feldspar-chlorite-biotite sills and dikes, and foliated, discontinuous and foliation-conformable plagioclase-actinolite-biotite-chlorite meta-igneous rocks (Murphy, 1997). Mafic rocks, interpreted to be analogous to those mapped by Murphy (1997), were also mapped by Abbott (1997) in the Upper Hart River area and have yielded a Cambrian U-Pb age from baddeleyite of 518.2 ± 2.9 Ma.

Sills of the Late Triassic Galena suite intrude the Keno Hill Quartzite and the underlying Earn Group, and are massive to foliated depending on their thicknesses, which can vary from less than 1 m to more than 100 m (Murphy, 1997; Read et al., 2020). Mineralogical variation is observed to be width dependent, where thinner foliated sills are composed of chlorite-actinolite-epidote (zoisite)-albite \pm stipnomelane, and wider sills with massive cores range from medium-grained metadiorite and metagabbro, to plagiophyric and/or hornblende-phyric variants (McOnie, 2016). A late Middle Triassic U-Pb age from baddeleyite of 232.2 ± 1.5 – 1.2 Ma was obtained from a Galena Suite gabbro in the Tombstone Range (Mortenson and Thompson, 1990).

Undeformed intrusions

Mid-Cretaceous intrusions of the Mayo suite (98–95 Ma; Rasmussen, 2013), as described by Hart et al. (2004), intrude metasedimentary rocks of the Hyland and Earn groups. The Mayo suite consists of metaluminous felsic to mafic plutons dominated by porphyritic quartz monzonite and are often cut by porphyritic, aplitic or pegmatitic felsic dikes and lamprophyre dikes. The Mayo suite is associated with gold mineralization such as the Eagle deposit (4.3 Moz Au [Measured and Inferred]; Harvey et al., 2023), which is hosted within the Mayo suite Dublin Gulch stock. A published U-Pb age from zircon of 94.1 ± 0.3 Ma (Yukon Geological Survey, 2023a)

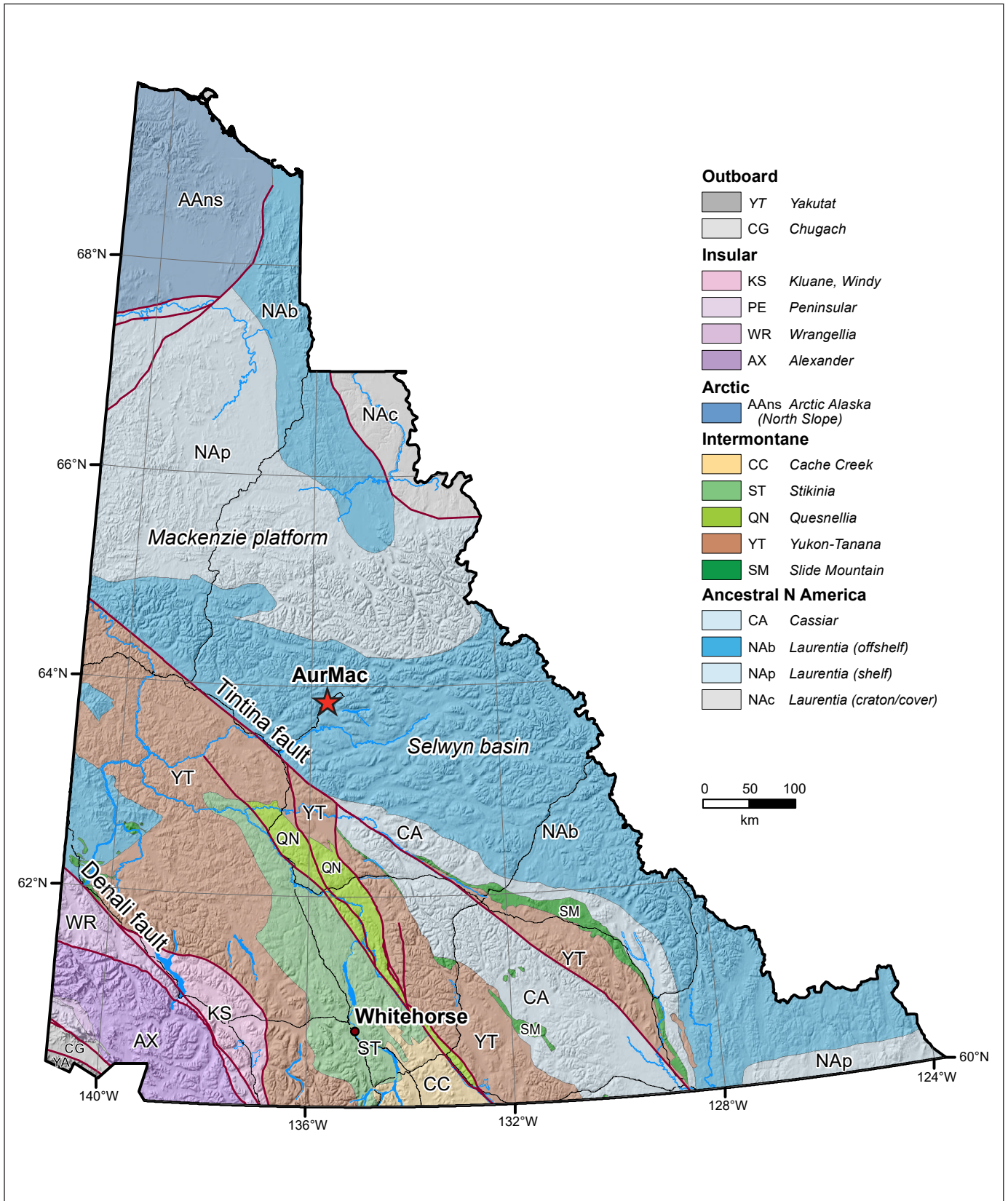


Figure 1. Location of the AurMac property displayed on the geological terrane map of the Yukon (after Yukon Geological Survey, 2020).

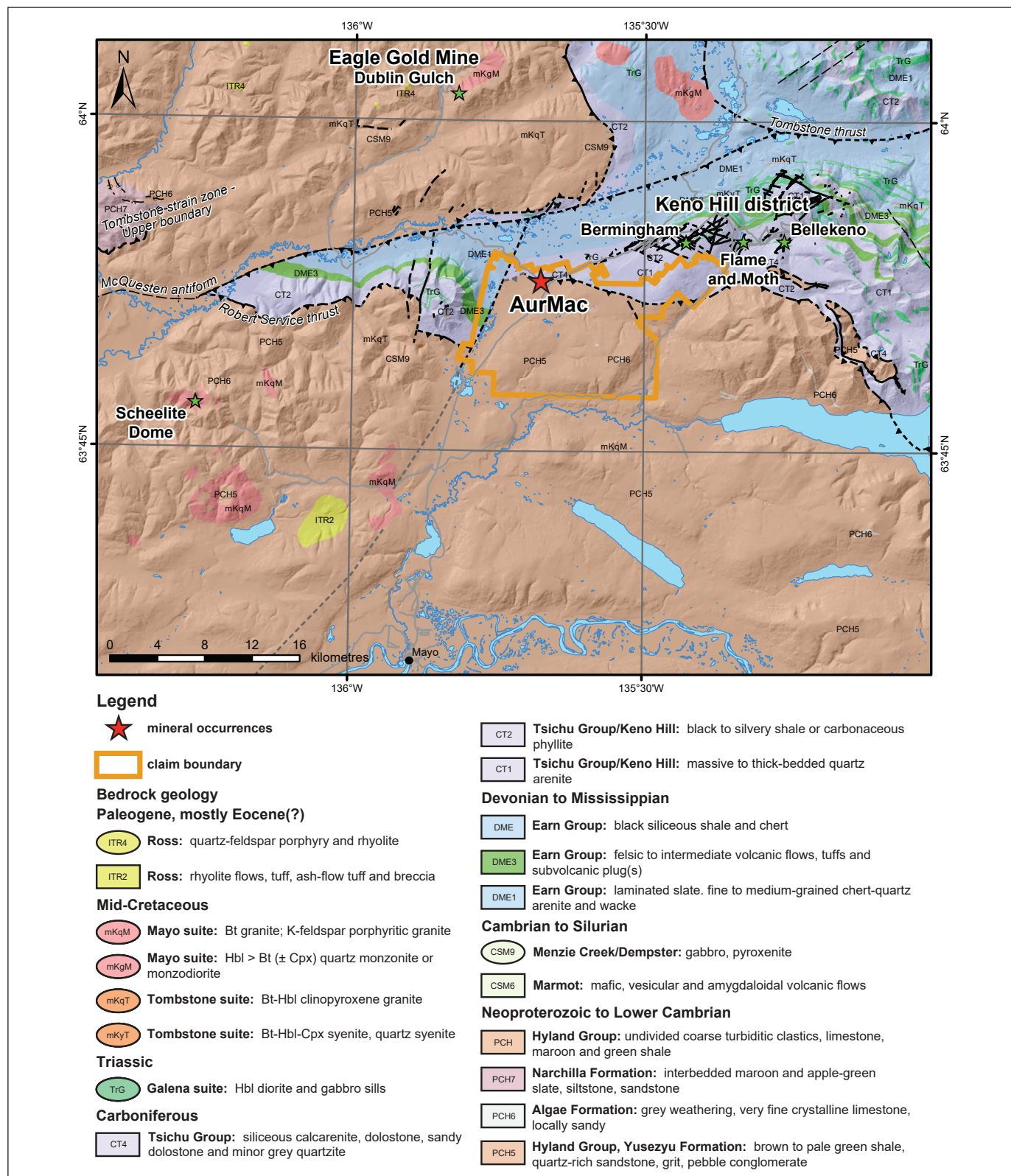


Figure 2. Bedrock geology map of the area surrounding the AurMac property. Nearby reduced intrusion-related gold systems include Dublin Gulch at the Eagle Gold Mine, and Scheelite Dome. Silver-lead-zinc mineralization occurs in the Birmingham, Bellekeno and Flame and Moth occurrences of the Keno Hill district (after Yukon Geological Survey, 2022).

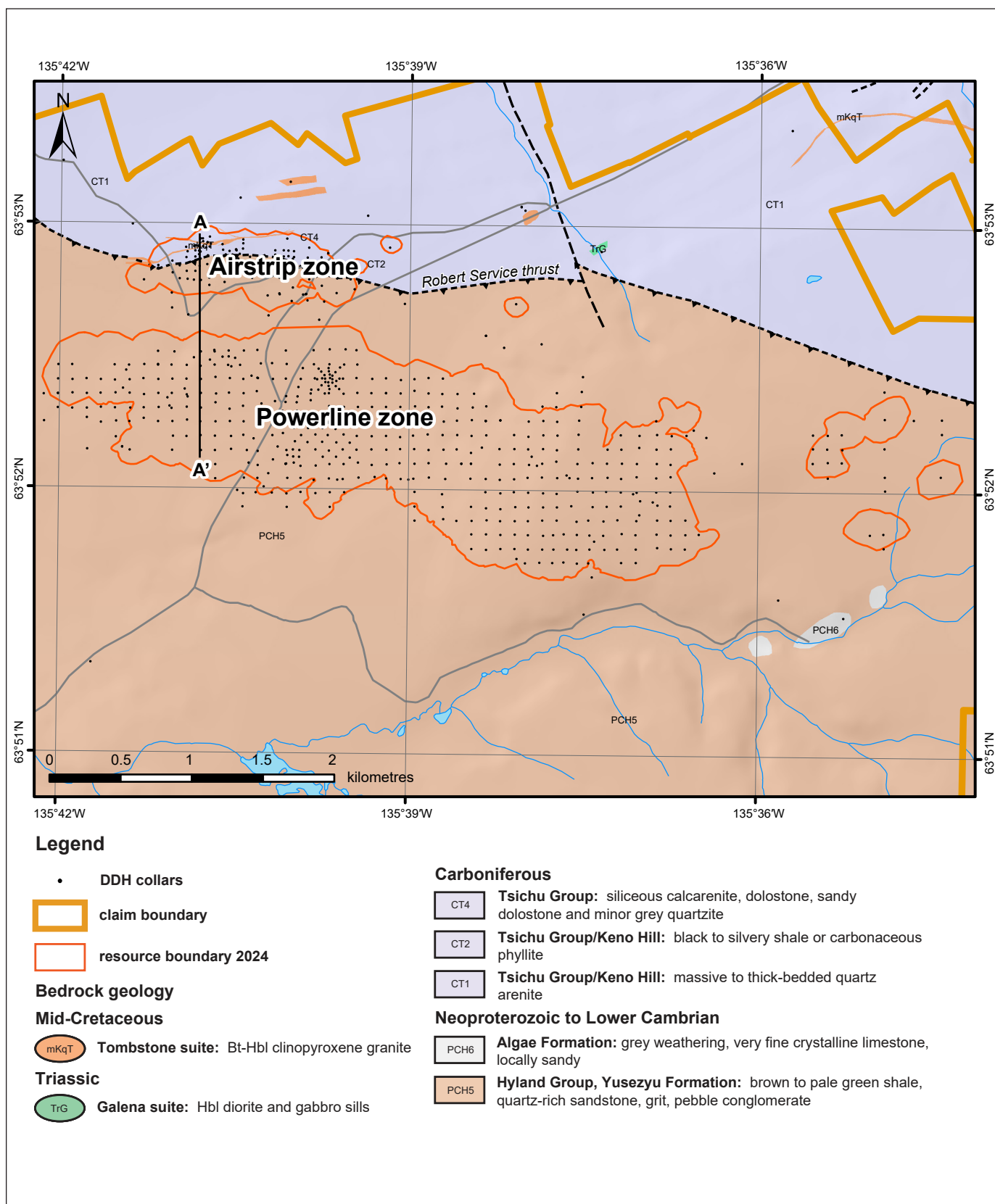


Figure 3. Diamond drillhole (DDH) collar map illustrating the location of relogged drillhole fence A–A' (466600 mE, UTM Zone 8) through the Airstrip and Powerline zones (after Yukon Geological Survey, 2022).

was calculated for an aplite dike crosscutting strata in the Airstrip zone, which is interpreted to belong to the Mayo suite.

The latest Cretaceous to earliest Paleocene (67–64 Ma; Murphy, 1997) McQuesten suite forms an east to northeast-trending belt situated between the Tintina fault and Sunshine Creek, and the known eastern limit is located approximately 45 km west of the AurMac property. This suite consists of reduced, peraluminous, medium to coarse-grained, megacrystic, potassium-feldspar-biotite \pm muscovite granite, and quartz monzonite stocks and batholiths. The McQuesten suite is associated with silver-tin mineralization in breccias (Murphy, 1997; Rasmussen, 2013).

Regional structure and deformation

Northward Jurassic to Early Cretaceous thrusting resulted in three prominent east-trending thrust faults in the northwestern Selwyn basin area (Mair et al., 2006). The Dawson thrust fault, the farthest north and structurally lowest of the thrusts, juxtaposes Selwyn basin strata over strata of the Mackenzie platform. This thrust is interpreted as a reactivated basin-bounding fault and the defining northern boundary of convergence-related ductile deformation (Mair et al., 2006). The Tombstone thrust, positioned above the underlying Dawson thrust, displaces Mississippian to Jurassic rocks above Upper Jurassic rocks in its footwall (Murphy, 1997). The Robert Service thrust (RST; Fig. 2), the most southerly of the three thrusts, is inferred to pass through the northern part of the AurMac property, where it juxtaposes the Late Proterozoic to Cambrian Hyland Group over the Mississippian to Permian(?) Keno Hill Quartzite and Devonian to Mississippian Earn Group (Murphy, 1997; Read et al., 2020).

Associated with these faults, and structurally overprinting the AurMac property, is the Tombstone strain zone (TSZ, Fig. 2). It is a region of increased deformation characterized by more prominent foliation, lenticular fabrics rather than bedding, mineral stretching lineations, isoclinal folding, asymmetric boudinage, and a slightly higher regional metamorphic grade (Murphy, 1997). The TSZ, extending laterally from the North Klondike River region in the west, to at least the Mt. Westman map area to the east, is defined by the Tombstone thrust at its base, and extends several kilometres upward through the Earn Group, Keno Hill Quartzite, and into the Yusezyu Formation of the Hyland Group along the base of the overlying RST sheet (Murphy, 1997).

The McQuesten antiform (Fig. 2) has its axial trace running north of the AurMac property, and is a steeply south-dipping, reverse-faulted, west-southwest-plunging antiform that folds the RST, Tombstone thrust and the TSZ (Murphy, 1997; Yukon Geological Survey, 2022). This structure is interpreted as the result of out-of-sequence fault propagation fold structures splaying from the Tombstone thrust, or a fault-bend fold resulting from thrusting over underlying ramps (Murphy, 1997, Mair et al., 2006).

The cessation of ductile deformation is interpreted to be closely represented by metamorphic muscovite $^{40}\text{Ar}/^{39}\text{Ar}$ cooling ages of 100.47 ± 0.40 Ma near Scheelite Dome, and 103.90 ± 0.54 Ma and 104.6 ± 2.00 Ma from the lower RST sheet, which mark cooling through approximately 350°C (Mair et al., 2006). Ductile deformation in the footwall of the Tombstone thrust fault is cross-cut by unfoliated mid-Cretaceous (ca. 98 to 88 Ma) intrusions (Mair et al., 2006).

Brittle deformation that postdates ductile deformation is characterized by north and north-northwest-striking sinistral strike-slip faults, conjugate northeast-trending dextral faults, and east-trending tensional structures (Hart et al., 2000; O'Dea et al., 2000; Stephens et al., 2000; 2004; Mair et al., 2006).

Methodology

In the summer of 2023, detailed core logging and targeted sampling was conducted at the AurMac logging facilities. Thirteen drillholes, totalling 3602 m, were relogged along a north-south section (section A–A' located along 466600 mE from 7082500 mN to 7084100 mN, UTM Zone 8; Fig. 3) through both the Airstrip and Powerline deposits. Polished thin sections were prepared by Vancouver Petrographics Ltd. on representative samples of magmatic units and mineralization observed at the AurMac deposits. Transmitted and reflected light petrography was used for characterization. Representative samples of mafic rocks were sent to ALS Canada Ltd. of North Vancouver, British Columbia, for whole-rock geochemical analyses using the PUL-42 sample preparation and CCP-PKG03 analytical packages. This package includes whole-rock analysis by x-ray fluorescence and trace-element analysis by lithium borate fusion.

Deposit geology

The AurMac property is situated along the regional trace of the RST where the Yusezyu Formation of the Hyland Group in the hanging wall overlies the Mississippian Sourdough Hill Member of the Keno Hill Quartzite in the footwall (Figs. 2 and 3). The area has been structurally overprinted by the TSZ (Fig. 2; Yukon Geological Survey, 2022) where the S_2 foliation and transposition fabric of the TSZ, as described by Murphy (1997) and Mair et al. (2006), defines the schistosity throughout the deposits. Being situated along the southern limb of the north-verging McQuesten antiform, a consistent, moderately south-dipping foliation (Fig. 4; Thornton et al., 2024) is observed across the AurMac deposits. Predominant, north-verging asymmetric folding observed during core logging in 2023 provides evidence that the host bedrock has not experienced significant structural thickening or repetition of strata through deposit-scale folding.

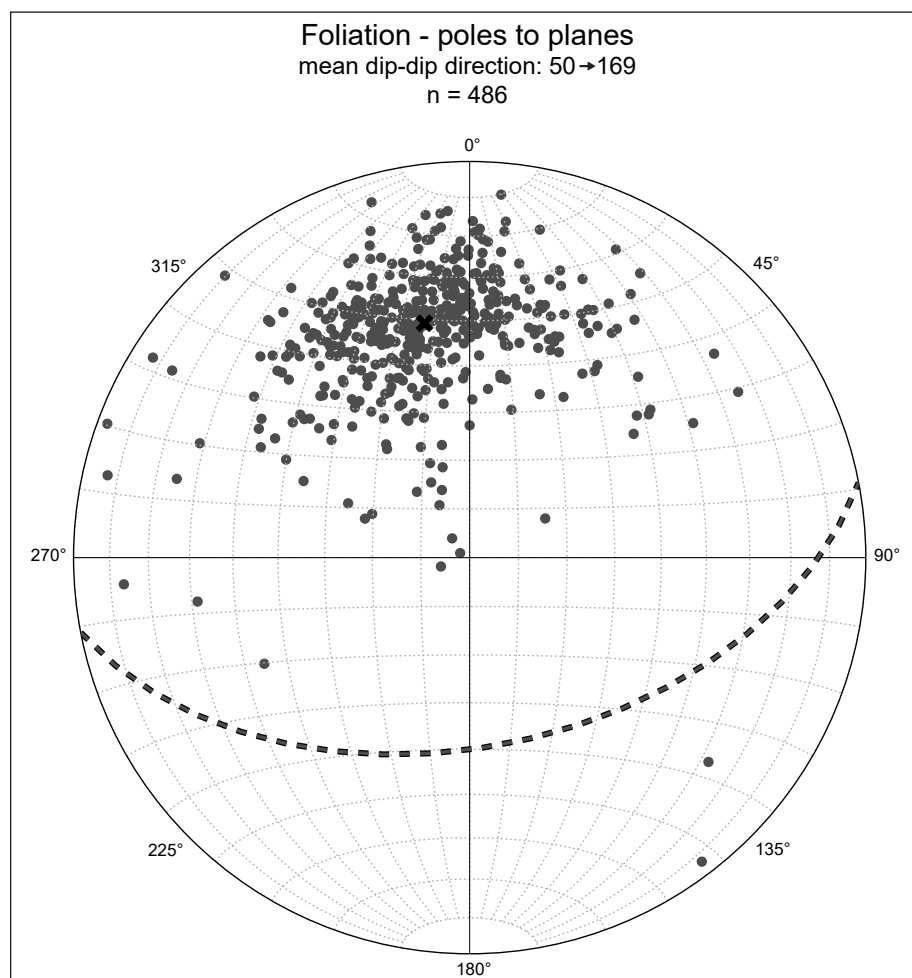


Figure 4. Stereonet displaying poles-to-planes of south-dipping foliation observed on the AurMac property.

Lithological units

Siliciclastic metasedimentary rocks

Micaceous metasedimentary rocks comprise the majority of host-rock lithologies at the AurMac deposits. The abundances of chlorite, white micas and muscovite in the metasedimentary lithologies vary across the deposits and are used to differentiate the various units, which are defined by the dominant mineralogy. Because of the variable nature of mica content in the metasedimentary rocks, the ideal end-member schist units described below are rare and lithologies with intermediate characteristics are more common.

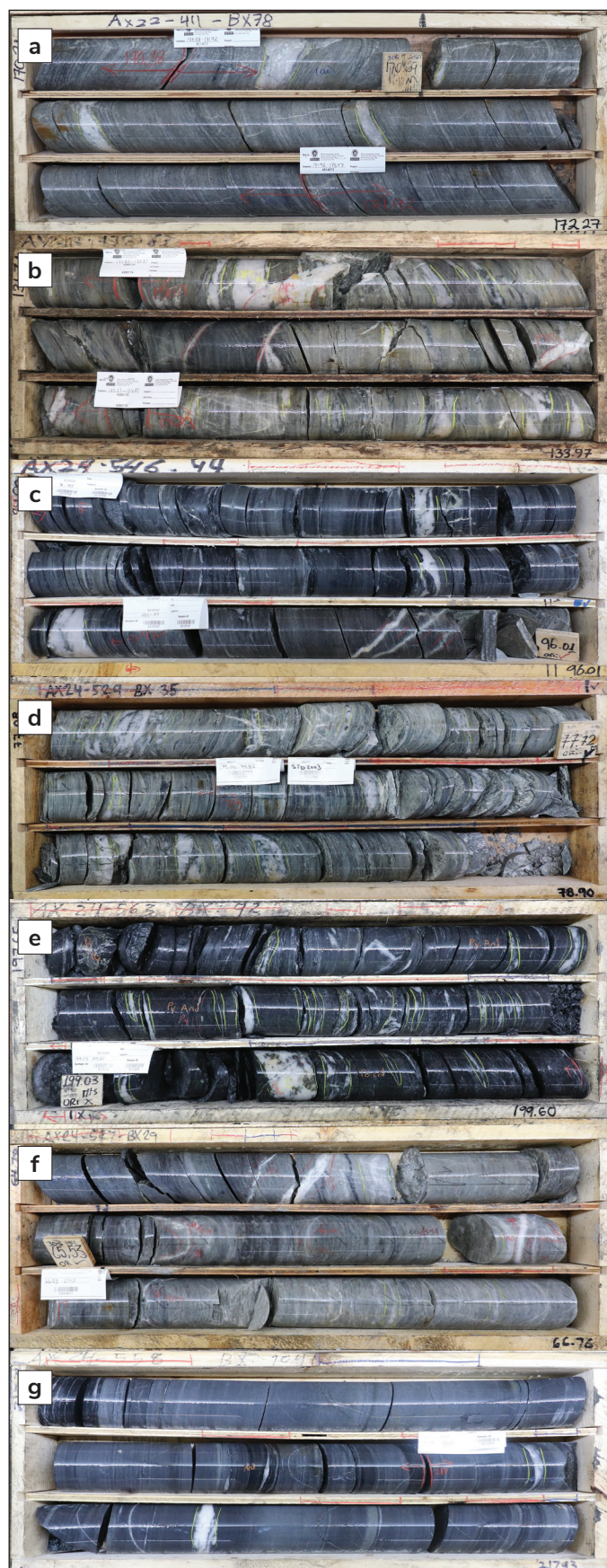
Mica-quartz schist

White mica-quartz \pm chlorite \pm biotite schist is a fine-grained, quartz-dominated lithology that typically exhibits a light to medium grey colour, but transitions to dark grey to black and brown where it is carbonaceous

and contains biotite, respectively (Fig. 5a). Micaceous laminae and bands are interspersed with planar sub-centimetre to sub-decimetre quartz segregations constituting 5–25% of the rock. Occasionally, 'gritty' bands of strained, coarse-grained (less than 3 mm), grey-black to light grey quartz clasts occur in sub-decimetre bands. The unit is more competent and resistant to scratching relative to mica-dominated schists, and silvery phyllitic foliation surfaces are exposed on broken surfaces. Where more mica-rich, the unit may host very fine to fine-grained disseminated pyrrhotite (less than 1%) and be weakly magnetic. White mica-quartz \pm chlorite \pm biotite schist is the most common unit in the Powerline zone and occurs in more shallow strata of the Airstrip zone.

Quartz-sericite schist

Quartz-sericite schist is a very fine grained white mica-dominated lithology characterized by its light beige-grey colour and relatively high fissility (Fig. 5b). Very narrow foliation is irregular, undulating



around quartz segregations, and tight to isoclinal folds are commonly observed. Sub-centimetre to sub-decimetres quartz segregations constitutes 5–20% of the unit and often appear as boudins or isoclinal rootless fold hinges with axial planes oriented parallel to foliation. Less than 5 mm, ovoid to blocky chloritoid porphyroblasts occasionally occur in white mica bands and have been completely retrograded to white mica and chlorite (Fig. 6a). Pyrrhotite, constituting less than 1% of the rock, occurs as very fine to fine-grained disseminations within micaceous bands contributing to the rocks being weakly to moderately magnetic where present. Quartz-sericite schist is identified in the Powerline and Airstrip zones.

Quartz-chlorite schist

Quartz-chlorite schist is a very fine grained, dark green-grey, chlorite-dominated lithology (Fig. 5c). Similar to the quartz-sericite schist, quartz-chlorite schist is relatively soft and fissile and has very narrow folia that undulate around quartz segregations and are commonly folded into tight to isoclinal folds. Quartz segregations generally constitute less than 10% of the rock and, like those observed in quartz-sericite schist, have sub-centimetre to sub-decimetres widths and occur as boudins and rootless isoclinal fold hinges. Cordierite porphyroblasts, although more frequent in carbonaceous units, occur in chlorite bands and appear as faint, 'ghostly', medium to dark grey, <8 mm ovoid to diamond-shaped porphyroblasts (Fig. 6b). Disseminated fine-grained pyrrhotite, comprising up to 1% of the rock, is more prevalent relative to muscovite-quartz and quartz-sericite schists and contributes to the schist's moderate to strong magnetism. Quartz-chlorite schist is identified in the Powerline zone and more shallow strata of the Airstrip zone.

Figure 5. Core photos from drillholes on the AurMac property. Core diameter is 71 mm (HTW). (a) Mica-quartz schist in drillhole AX-22-411. (b) Quartz-sericite schist in drillhole AX-23-438. (c) Quartz-chlorite schist in drillhole AX-24-546. (d) Quartz-sericite-chlorite and quartz-chlorite-sericite schist in drillhole AX-24-546. (e) Graphitic schist in drillhole AX-24-563. (f) Quartzite in the Powerline zone from drillhole AX-24-559. (g) Quartzite in the Airstrip zone from drillhole AX-24-558.

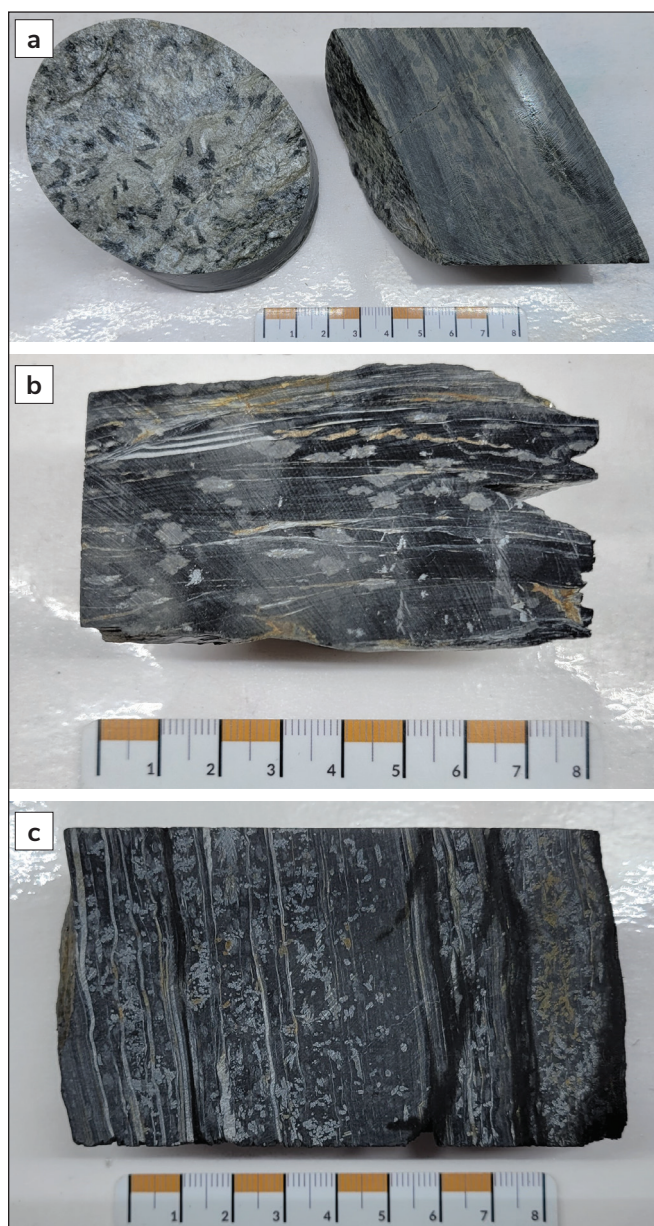


Figure 6. Examples of minerals from the AurMac property. All scales are in centimetres. **(a)** Chloritoid porphyroblasts in quartz-sericite schist. **(b)** Cordierite porphyroblasts in graphitic schist. **(c)** Andalusite porphyroblasts in graphitic schist.

Quartz-sericite-chlorite and quartz-chlorite-sericite schist

Quartz-chlorite-sericite and quartz-sericite-chlorite schists represent an intermediate facies between the quartz-chlorite and quartz-sericite schists. These lithologies are very fine grained and characterized by alternating or interfingering dark green-grey chlorite, beige to grey-white mica, and quartz-rich bands and laminae (Fig. 5d). As with other mica-dominated units,

quartz-chlorite-sericite and quartz-sericite-chlorite schists are very soft and fissile. Folded and boudinaged quartz segregations, constituting approximately 10% of the rock, are similar to those observed in chlorite and sericite-dominated schists. Chloritoid and cordierite porphyroblasts, as observed in quartz-sericite and quartz-chlorite schists, occur in white mica and chlorite bands, respectively (Figs. 6a, b). Very fine grained disseminated pyrrhotite, which is most common in chlorite-rich bands, constitutes less than 1% of the rock and contributes to the unit's moderate to strong magnetism. Quartz-chlorite-sericite and quartz-sericite-chlorite schists are identified in the Powerline zone.

Graphitic schist

Quartz-rich graphitic schist is present in the Powerline zone as metre-scale horizons and found in larger decametre-scale horizons in the Airstrip zone. This lithology is very fine grained and consists predominantly of black graphite laminae and bands, which are interspersed with grey-black carbonaceous quartz and occasional chlorite bands and laminae (Fig. 5e). Among the schist varieties at AurMac, graphitic schist is the most fissile and soft, and is notably prone to faulting resulting in prominent rubble and gouge-rich fault zones. Quartz segregations within the graphitic schist are similar to those in mica-dominated schists, occurring as sub-centimetre to sub-decimetre boudins and rootless isoclinal fold hinges. Fine to coarse-grained andalusite porphyroblasts are observed at depth in the Airstrip zone and appear as white, sub-centimetre radiating columnar clusters or as square cross sections of individual crystals (Fig. 6c). The unit hosts less than 1% fine-grained euhedral pyrite and up to 5% very fine grained to blebby pyrrhotite occasionally intergrown with chalcopyrite, which contributes to a pervasive, moderate to strong magnetism that differentiates the unit from other schists. Very fine grained disseminated carbonate is more common in graphitic schists in the Airstrip zone, where reactions to dilute muriatic acid are moderately vigorous. Quartz-graphite schist is identified in the Powerline and Airstrip zones.

Quartzite

Quartzite is present in both the Powerline and Airstrip zones, although it is more prevalent and visually distinct in the Airstrip zone.

In the Powerline zone, quartzite units are relatively uncommon and characterized by their fine to coarse-grained texture, light grey colour with dark grey to black

carbonaceous banding, and vitreous texture (Fig. 5f). Relative to mica-rich schists, quartzite exhibits wider banding with more consistently planar foliation, and bands of coarse-grained, rounded grey to dark-grey quartz clasts or 'grit' are a common feature. Quartzite units have the highest competency among the units in the Powerline zone and in drill core, and have scratch-resistant polished surfaces. Quartzite units are less fissile than mica-bearing schists, and fracture surfaces expose uneven, mica-poor surfaces. Quartz segregations in these units are similar to that found in schists, comprising less than 10% of the rock (rarely up to 20%), and have sub-centimetre to sub-decimetres widths. Disseminated fine-grained to blebby pyrrhotite is most often absent, which differentiates quartzite horizons from more quartz-rich schist units.

In the stratigraphically deeper parts of the Airstrip zone, quartzite units are very fine to fine grained, are carbonaceous with a medium grey to black colour, and lack the coarse-grained 'gritty' bands observed in quartzite of the Powerline zone (Fig. 5g). Graphitic partings and bands are common and host radiating, white, fine to coarse-grained andalusite porphyroblasts like those observed in graphite schists (Fig. 6c). Mica content in the Airstrip zone quartzite units is notably elevated relative to quartzite in the Powerline zone, and where present, is associated with zones of increased fissility. These quartzite units exhibit high competency and resistance to scratching, similar to those found in the Powerline zone. Horizons of very fine grained carbonate disseminations are more common in the Airstrip zone quartzite and react moderately with dilute muriatic acid. Disseminated, very fine grained to blebby pyrrhotite occurs in more carbonaceous and calcareous horizons, and is associated with weak to moderate magnetism. Brecciation is prevalent in the Airstrip zone quartzite units, characterized by an iron carbonate matrix hosting fine to coarse-grained sphalerite ± galena ± arsenopyrite ± pyrite ± pyrrhotite.

Calcareous metasedimentary rocks

Calcareous units are found throughout the AurMac deposits but are notably more abundant in the Airstrip zone, where gold mineralization is primarily associated with skarn horizons (Gray and Thom, 2021). Calcareous units are differentiated by their carbonate content and varying degrees of silicification and alteration, and rarely have sharp, well-defined contacts.

Calcareous schist

Calcareous schist units, which are defined by an elevated concentration of limey horizons within micaceous schists, are observed in both the Powerline and Airstrip zones. The mineralogical composition of these units varies and ranges from being dominated by quartz, chlorite or white mica. This unit exhibits similar colour, foliation, competency and quartz segregation abundances with previously described schists. The primary distinction made between calcareous schists and previously described metasedimentary units is based on elevated, very fine to fine-grained carbonate disseminations and limey, fine-grained laminae and banding, which contribute to a pervasive, moderate to strong reaction with dilute muriatic acid. Disseminated fine-grained to blebby pyrrhotite is more abundant in calcareous schists, comprising up to 2% of the units, and results in these units having moderate to strong magnetism. Calcareous schists are identified throughout the AurMac deposits but are more prevalent in the Airstrip zone.

Marble

Marble is notably more widespread in the Airstrip zone compared to the Powerline zone and is visually distinct between the two deposits.

In the Powerline zone, foliated marble is fine to medium grained and ranges in colour from white to blue-grey. Powerline zone marble is predominantly composed of calcite, and has less than 10% fine-grained quartz and very fine grained micaceous laminae (Fig. 7a). Individual limestone horizons typically do not exceed 5 m in width and are often intercalated with dark green to grey, quartz-chlorite schist or beige-grey, quartz-white mica schist. These marble horizons possess higher competency and hardness relative to schists and are most readily identified by their vigorous reaction to dilute muriatic acid, having the strongest reaction relative to all other units. Although laminae and banding are generally planar, well-developed, open to narrow folding can be observed. Sub-centimetre quartz-carbonate segregations are rare, comprising up to 5% of the unit.

Marble horizons are more extensive in the Airstrip zone and individual band thicknesses average approximately 2 m and occasionally reach up to 10 m. In contrast to marble in the Powerline zone, marble in the Airstrip zone is fine grained and has chlorite, white mica and graphitic partings contributing to its grey, green and black hues (Fig. 7b). Although marble horizons in

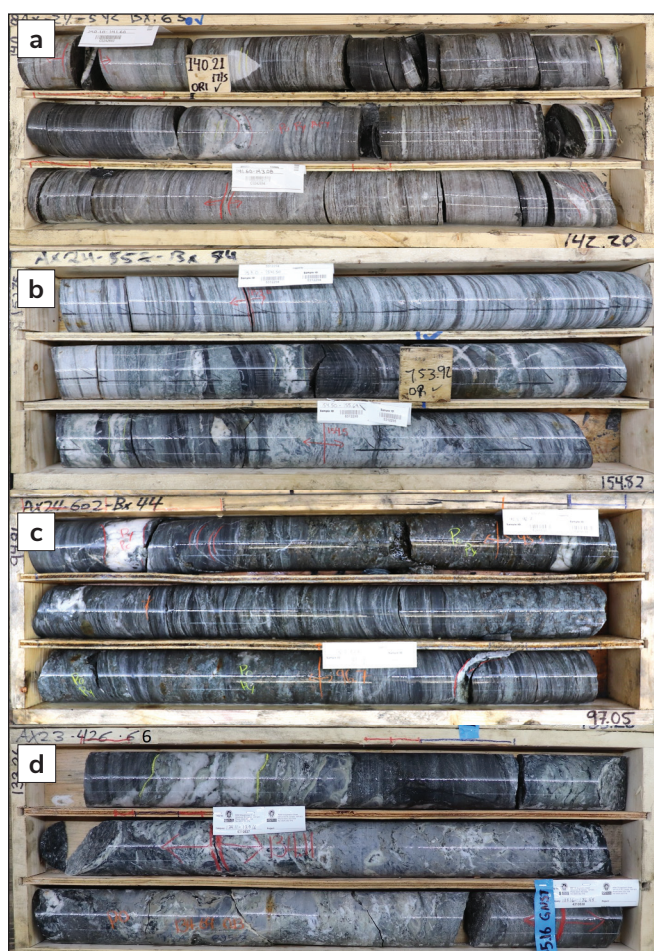


Figure 7. Core photos from drillholes on the AurMac property. Core diameter is 71 mm (HTW). **(a)** Marble in the Powerline zone from drillhole AX-24-542. **(b)** Marble in the Airstrip zone from drillhole AX-24-558. **(c)** Alternating foliated calc-silicate and massive skarn from drillhole AX-24-558. **(d)** Very fine grained calcareous quartzite in drillhole AX-23-426.

the Airstrip zone are relatively competent, they are comparatively less so than those in the Powerline zone due to their higher mica content. Centimetre to sub-decimetre-wide quartz-carbonate segregations are more abundant in the Airstrip zone marble, comprising up to 10% of the unit.

Foliated calc-silicate rocks

In the Airstrip zone and less frequently in the Powerline zone, foliated, fine-grained, banded to laminated calc-silicate rocks (Fig. 7c) occur along margins of marble, calcareous schist and massive skarn horizons; they typically have widths of <2 m. Calc-silicate hornfels

are green-grey, grey-brown or beige, and feature wispy white mica and chlorite laminae, which separate massive, light to medium-grey-green lenses of fine-grained calcite, quartz and epidote-clinozoisite. The competency of these calc-silicate rocks varies with zones of increased natural fracturing associated with elevated mica content. Foliated calc-silicate horizons host up to 2% fine-grained disseminated pyrrhotite, trace chalcopyrite and rare fine to medium-grained scheelite. Where pyrrhotite is present, the unit is moderately to strongly magnetic. Reactions with dilute muriatic acid are moderate to strong, and primarily occur along the calcite-bearing bands between white mica folia.

Massive skarn

Skarn horizons are most prominent in the Airstrip zone where they can reach several metres in width. In contrast, skarn horizons in the Powerline zone are scarce and widths rarely exceed 1 m. Skarn horizons are characterized by their grey to brown colour, abundant sulphide content, intense silicification, high competency and massive fine to coarse-grained texture (Fig. 7c). Sulphides in skarn horizons, sometimes exceeding 10% of the unit, consist of net-textured to blebby pyrrhotite, lesser fine to medium-grained pyrite and arsenopyrite, and very fine to fine-grained chalcopyrite. Due to the high pyrrhotite content, skarn horizons are the most strongly magnetic of all units observed on the AurMac property. Carbonate content is low in these units and when tested with dilute muriatic acid, reactions are generally weak to moderate, and observed sporadically.

Petrographic analysis reveals that skarn units have a quartz-calcite matrix surrounding equant, fine to medium-grained clinopyroxene; fine-grained, elongate and fibrous amphibole; and fine-grained feldspar. It also contains fine to coarse-grained scheelite, fine-grained biotite and chlorite, and rare fine-grained garnet.

Very fine grained calcareous quartzite(?)

Very fine grained, variably calcareous quartzite(?) horizons are only observed in the Powerline zone and occur as distinct highly competent, light grey to black, very fine grained, massive calcareous and siliceous rocks, and widths rarely exceed 1 m (Fig. 7d). Carbonate content is lower than that of marble, and when tested with dilute muriatic acid, exhibits a pervasive, weak to moderately vigorous reaction. Brecciation is common in these quartzite horizons and typically occurs as mosaic breccias with black intraclastic crackle brecciation. Calc-

silicate alteration, where present, can be near pervasive, and is texturally destructive, resulting in a green-grey to brown mottled colouration. Unlike in previously described units, quartz segregations are absent. Fine to medium-grained pyrrhotite disseminations and blebs are present where calc-silicate alteration occurs, comprising up to 1% of the unit, and are associated with moderate to strong magnetism. Unit margins are generally obscured by alteration; however, where unaltered, they exhibit sharp and conformable contacts.

Magmatic rocks

Mafic rocks

Foliated mafic units at the AurMac property are confined to the Powerline zone and occur as fine to medium-grained sets of sub-metre thick bands that rarely exceed 20 m in true thickness. The mafic units are characterized by a dark green to grey and brown banded appearance, and contain fine-grained pervasive chlorite, very fine grained disseminated carbonate, and brown, fine-grained laminated to banded biotite (Fig. 8a). The rocks are relatively competent compared to surrounding schists and exhibit minimal natural fracturing. Carbonate is generally pervasive and has a weak to moderately vigorous reaction with dilute muriatic acid. Key characteristics that assist with differentiating the unit from others include the absence of quartz segregations, the presence of pervasive, very fine to fine-grained pyrrhotite associated with moderate to strong magnetism, a darker colour relative to metasedimentary schists, and contacts that are sharp and conformable to foliation.



Figure 8. Core photos from drillholes. Core diameter is 71 mm (HTW). (a) Mafic sills/volcanic units in drillhole AX-24-528. (b) Aplite dike in drillhole AX-24-598.

Petrographic analysis reveals that the mafic units have a well-developed foliation defined by mineralogically alternating layers. These layers consist of a) fine-grained hornblende (<5%), biotite (10%) and fine-grained to blebby pyrrhotite (<5%) set in a very fine grained chlorite matrix and b) layers of fine to medium-grained biotite (10%) and fine-grained chlorite (10%) embedded in a very fine to fine-grained quartz-white mica matrix (Fig. 9).

Aplite dike

Crosscutting the schists in the Airstrip zone is a light grey to pale green, massive, fine to medium-grained quartz-pyrrhotite aplite dike (Fig. 8b). This dike is characterized by its near-pervasive carbonate alteration, exhibiting a weak to moderate reaction with dilute muriatic acid, and sparse sub-centimetre quartz phenocrysts. The aplite dike dips steeply, approximately 70° toward the south (strike of 175°) and bifurcates as it extends west from section 466600 mE (Fig. 3). The average true width, calculated from drill core intercepts, is approximately 3.5 m, but true widths can range from less than 2 m up to approximately 26 m in drillhole MQ-20-66.

Petrography reveals the dike consists of weakly strained less than 2 mm quartz phenocrysts (40%) hosted in a highly altered, fine-grained muscovite to sericite (50%;

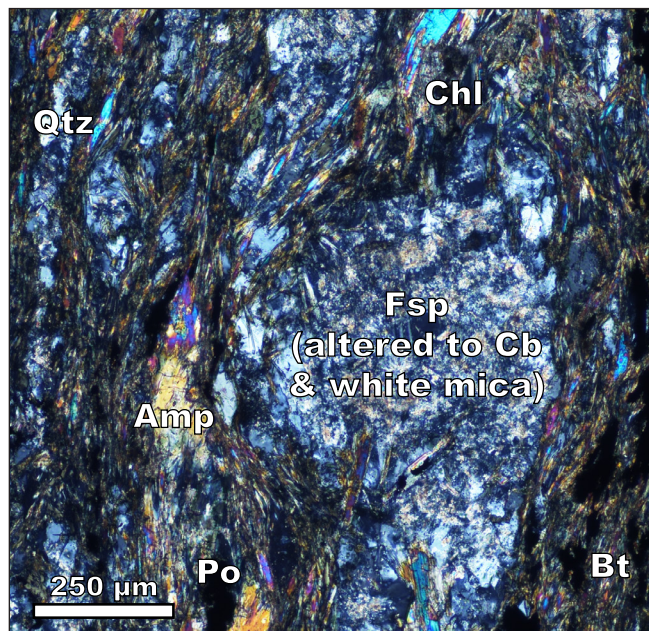


Figure 9. Cross-polarized transmitted light photomicrograph displaying an example of mafic rocks composed of amphibole (Amp), biotite (Bt), chlorite (Chl), quartz (Qtz), pyrrhotite (Po; opaque), and feldspar (Fsp) partly altered to carbonate (Cb) and white mica.

after feldspar?) and carbonate (10%) groundmass (Fig. 10). The aplite hosts less than 1% fine to medium-grained scheelite and up to 1% disseminated sulphides consisting of fine to medium-grained arsenopyrite, and fine-grained pyrite, pyrrhotite and sphalerite.

Geochemical analyses

Whole-rock geochemical analyses were conducted on the mafic rocks observed in the Powerline zone to characterize their compositions, rare earth element (REE) signatures, and for correlation with potentially analogous mafic units mapped outside of the AurMac property.

Zirconium (Zr) to titanium (Ti) versus niobium (Nb) to yttrium (Y) immobile element plots (Fig. 11; modified from Pearce, 1996) reveal that the mafic rocks at AurMac exhibit alkali basaltic compositions. Chondrite-normalized REE patterns (Fig. 12; Anders and Grevesse, 1989) of the mafic units exhibit a signature transitional between oceanic island basalts (OIB) and enriched mid-ocean ridge basalts (E-MORB; Sun and

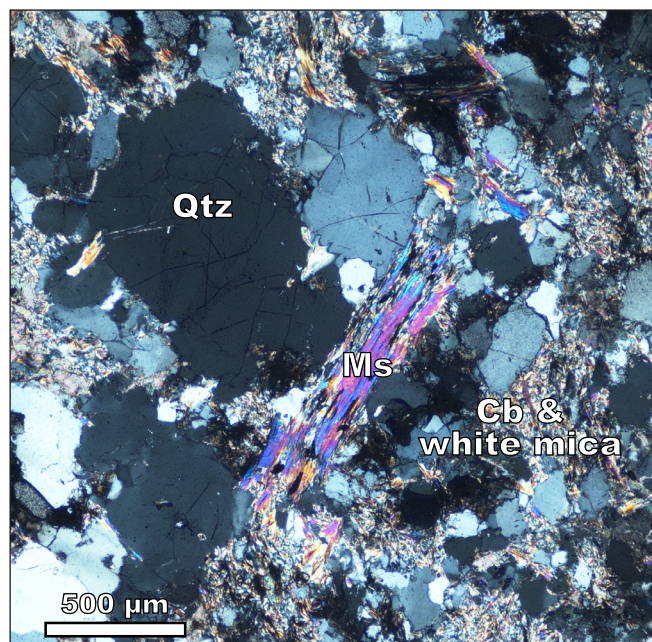


Figure 10. Cross-polarized transmitted light photomicrograph of the aplite dike composed of quartz (Qtz) and muscovite (Ms) in a matrix that is intensely altered to carbonate (Cb) and sericite (white mica).

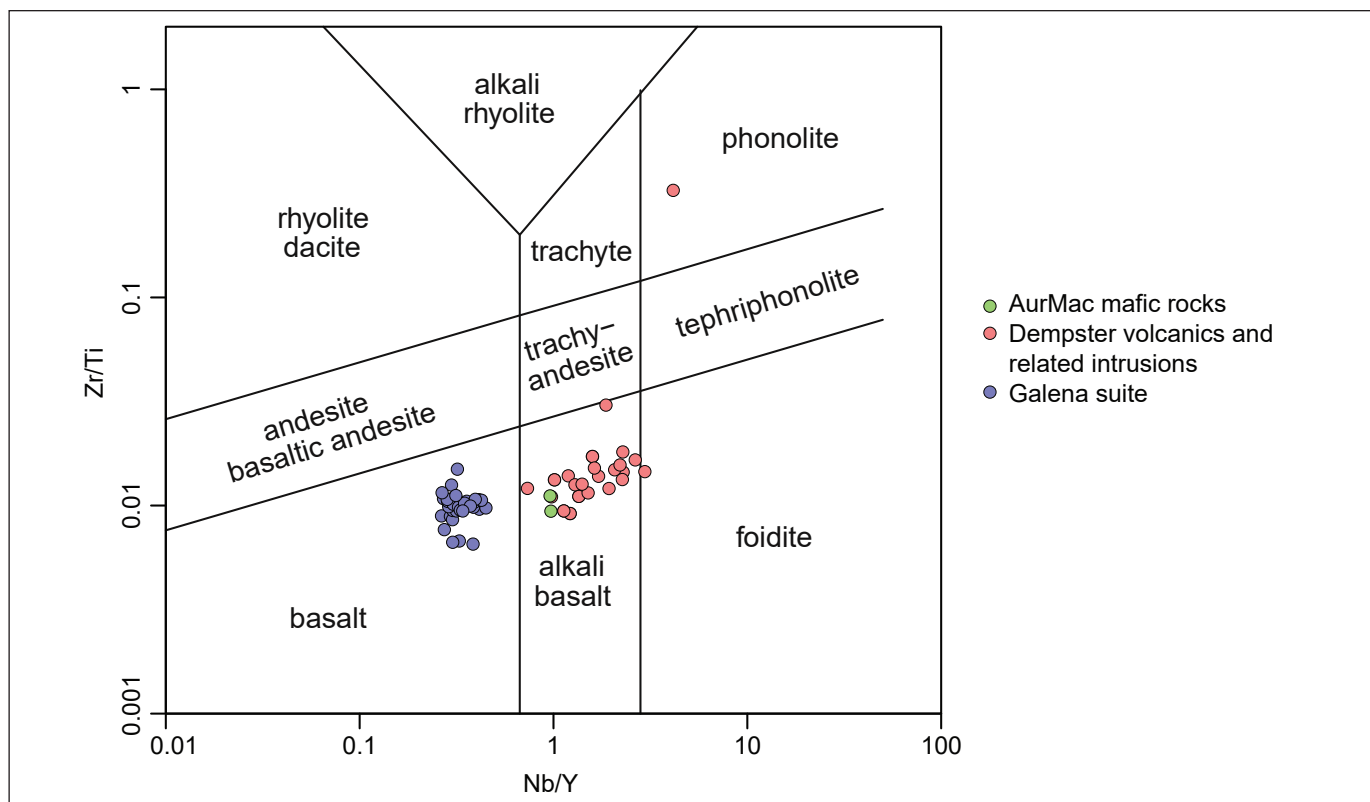


Figure 11. Zirconium (Zr) to titanium (Ti) versus niobium (Nb) to yttrium (Y) immobile element plot (modified from Pearce, 1996) of mafic units at AurMac (this study), Triassic Galena suite sills (Yukon Geological Survey, 2023b), and Dempster volcanics and related intrusions (Yukon Geological Survey, 2023b).

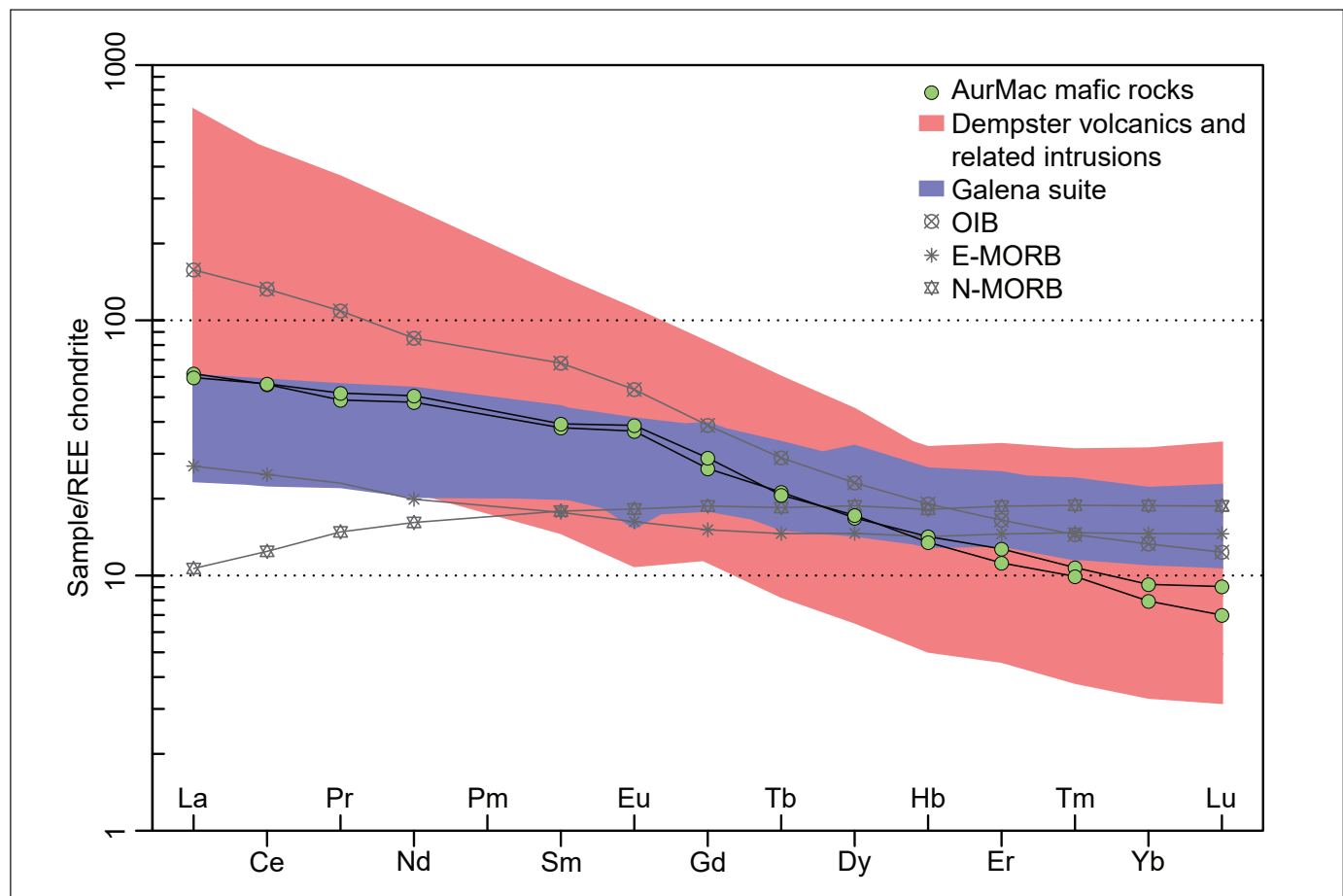


Figure 12. Chondrite-normalized REE plot (Anders and Grevesse, 1989) of mafic units at AurMac (this study), Triassic Galena suite sills (Yukon Geological Survey, 2023b), and Dempster volcanics and related intrusions (Yukon Geological Survey, 2023b). E-MORB: enriched mid-ocean ridge basalt; N-MORB: normal mid-ocean ridge basalt; OIB: oceanic island basalt.

McDonough, 1989), and a stronger enrichment in light REEs relative to heavy REEs.

Mafic units at AurMac could correspond to two varieties of mafic intrusions that have been mapped in the McQuesten, Mayo, Clark Lakes and Hart River map areas, including the Triassic Galena suite sills that intrude the Keno Hill Quartzite and underlying Earn Group (McOnie, 2016; Read et al., 2020), and intermediate to mafic Cambro-Ordovician intrusions and volcanic rocks (Dempster Volcanics), mapped within, and conformably overlying, the Hyland Group (Roots and Abbott, 1988; Abbott, 1997; Murphy, 1997; Skipton and Maw, 2021; Yukon Geological Survey, 2023b). The geochemical signatures of the mafic units at AurMac most closely resemble, and have been correlated with, the Cambro-Ordovician intrusions and volcanic rocks. This correlation has resulted in the interpretation that metasediment rocks hosting the

Powerline zone belong to the Hyland Group and are situated in the hanging wall of the RST (Fig. 13).

Cross sections and unit correlation

Interpolation of previously described lithological units between drillholes relogged along the 466000 mE fence results in the cross section in Figure 13. A correlation of units observed at the AurMac deposits has also been made with the geology published in reports and maps from the nearby Keno Hill district (Fig. 14; Read et al., 2020). Metamorphic isograds based on porphyroblasts observed in drill core are presented in Figure 15. These porphyroblasts, grading from chloritoid in the south, to cordierite, then andalusite in the north highlight an increasing metamorphic grade to the north.

Siliciclastic metasedimentary rocks observed along the southern part of the section in the Powerline zone are

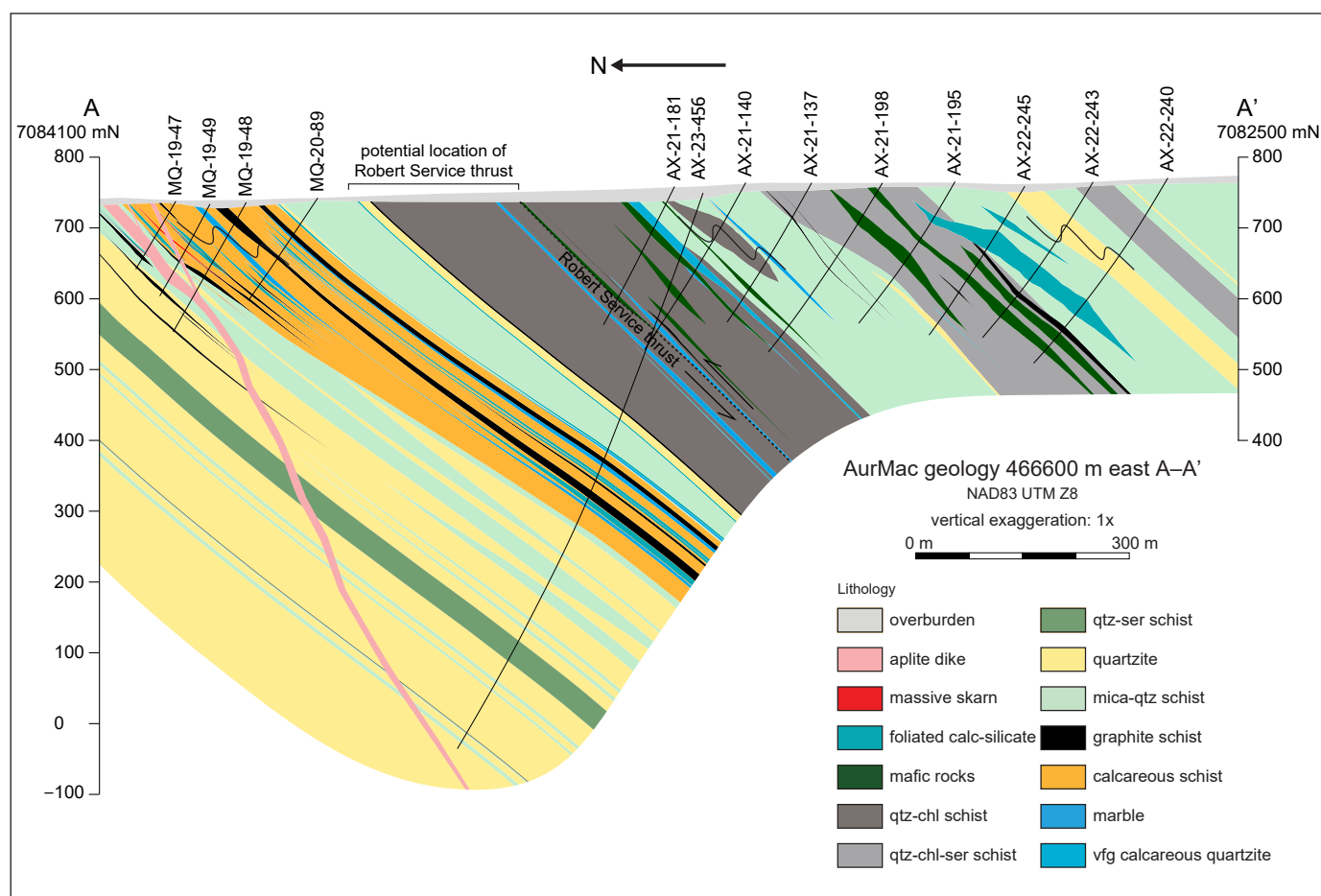


Figure 13. Geological cross section A–A' along 466600 mE from 7084100 mN to 7082500 mN (UTM Zone 8) through both the Airstrip and Powerline zones. Chl: chlorite, qtz: quartz, ser: sericite, vfg: very fine grained.

dominated by variable 'gritty' mica-quartz and chlorite and white mica-rich quartz-mica schists, and consist of subordinate graphitic schist, variable calc-silicate-altered marble, and quartzite. These units are correlated with Hyland Group rocks of the Yusezyu Formation (PY) in the Keno Hill district where they are described as chlorite-muscovite schists, quartz grain, gritty schists and metagrit. The lower limit of the Hyland Group and stratigraphically highest potential position of the RST in the Powerline zone is defined by the stratigraphically lowest occurrence of foliated mafic rocks, which have been correlated through whole-rock geochemistry with Cambro-Ordovician (Cd) mafic rocks mapped within the Hyland Group (Figs. 11 and 12; Skipton and Maw, 2021).

Quartzite observed in the lower stratigraphic levels of the Airstrip zone are correlated with the Upper Quartzite unit (MSq) in the Keno Hill district. These units share similar grey to dark grey colours, graphitic partings and fissile fracturing.

Calcareous metasedimentary rocks are observed above the Upper Quartzite in the Airstrip zone and include variably calc-silicate-altered micaceous marble and calcareous schists. These carbonate-rich horizons are flanked by variably calcareous, andalusite-bearing carbonaceous to graphitic schists, which are correlated with grey, locally phyllitic limestone (MSIs), and locally limey graphitic and siliceous schists (MSg), respectively, of the Sourdough Hill Member mapped in the Keno Hill district.

Above the calcareous metasedimentary rocks in the Airstrip zone, and below the mafic units observed in the Powerline zone, are horizons of green-grey chlorite and quartz-dominated schists. These rocks have been correlated with undifferentiated green and grey-green schists of the Sourdough Hill Member (MSC) although the extent of potential intercalation with overlying Hyland Group along the RST is unknown.

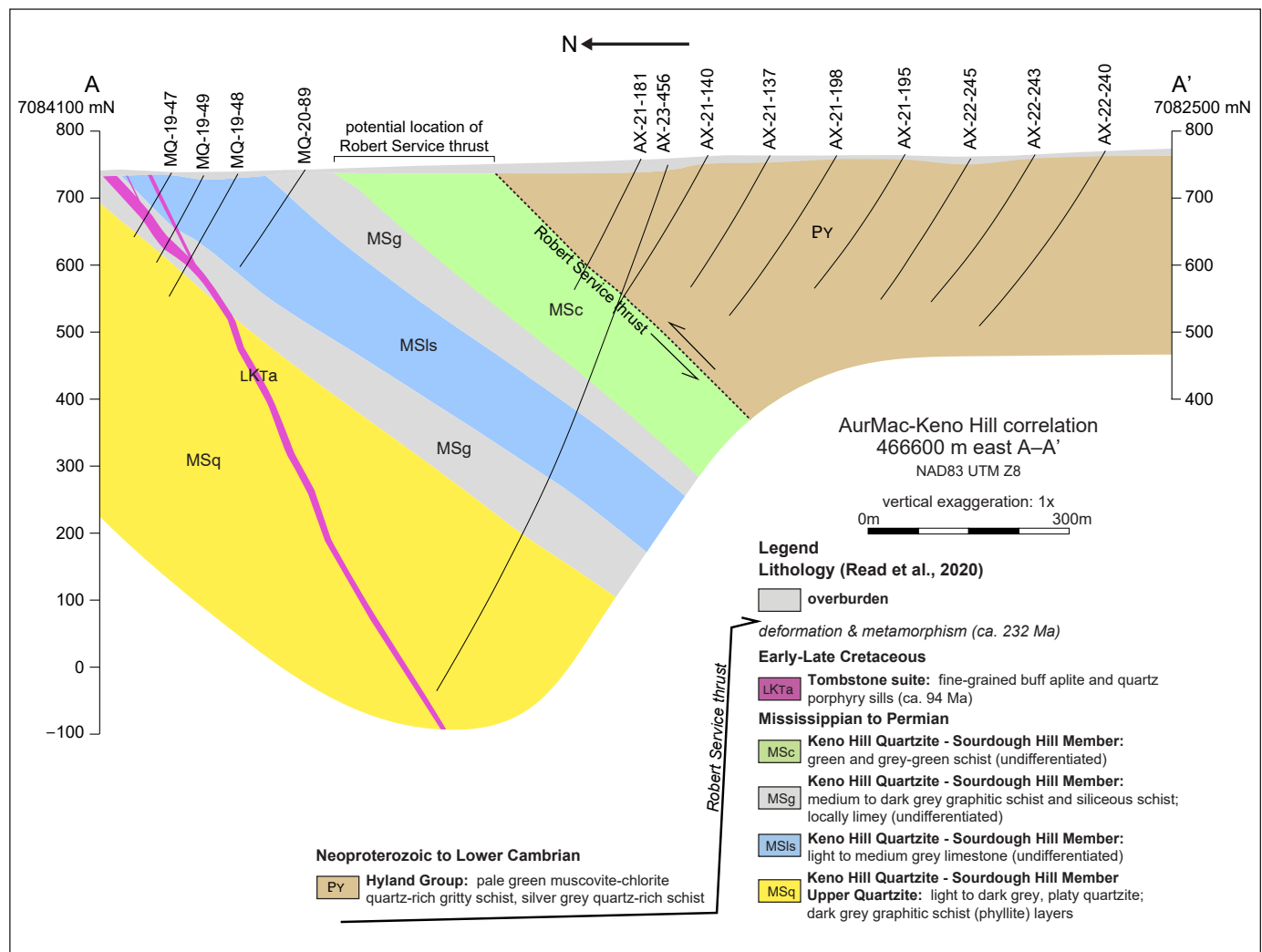


Figure 14. Cross section A–A' along 466600 mE from 7084100 mN to 7082500 mN (UTM Zone 8) illustrating unit correlations made with Keno Hill district geology from Read et al. (2020).

The quartz-phyric aplite dike, crosscutting strata in the Airstrip zone along the north end of the section, is correlated with mid-Cretaceous aplite and quartz porphyry sills mapped in the Keno Hill district (LKTa).

Mineralization styles and alteration

Gold mineralization within the AurMac property is characterized by two primary styles consisting of lithologically controlled carbonate replacement skarn, found primarily in the Airstrip zone, and structurally controlled sheeted veining found primarily in the Powerline zone. Although currently considered economically insignificant, silver-lead-zinc mineralization postdates and crosscuts gold mineralization throughout the deposits at AurMac.

Sheeted veins

Gold mineralization in the Powerline deposit is predominantly associated with arrays of sheeted quartz-carbonate ± albite veins that crosscut all fabrics related to ductile deformation and typically host less than 5% sulphides consisting of arsenopyrite-pyrite ± pyrrhotite ± chalcopyrite ± sphalerite ± lead-bismuth sulphosalts. Vein widths range from millimetre to decimetre-scale, and have an average width of less than 2 cm. Vein density appears rheologically controlled, and higher vein densities are associated with more siliceous host rocks, and in mineralized zones, they vary from approximately one to more than five veins per metre (Fig. 16a). Sheeted veins within the Powerline deposit are consistently shallowly dipping approximately 15° to the north (Fig. 17), and occur clustered in stacked horizons.

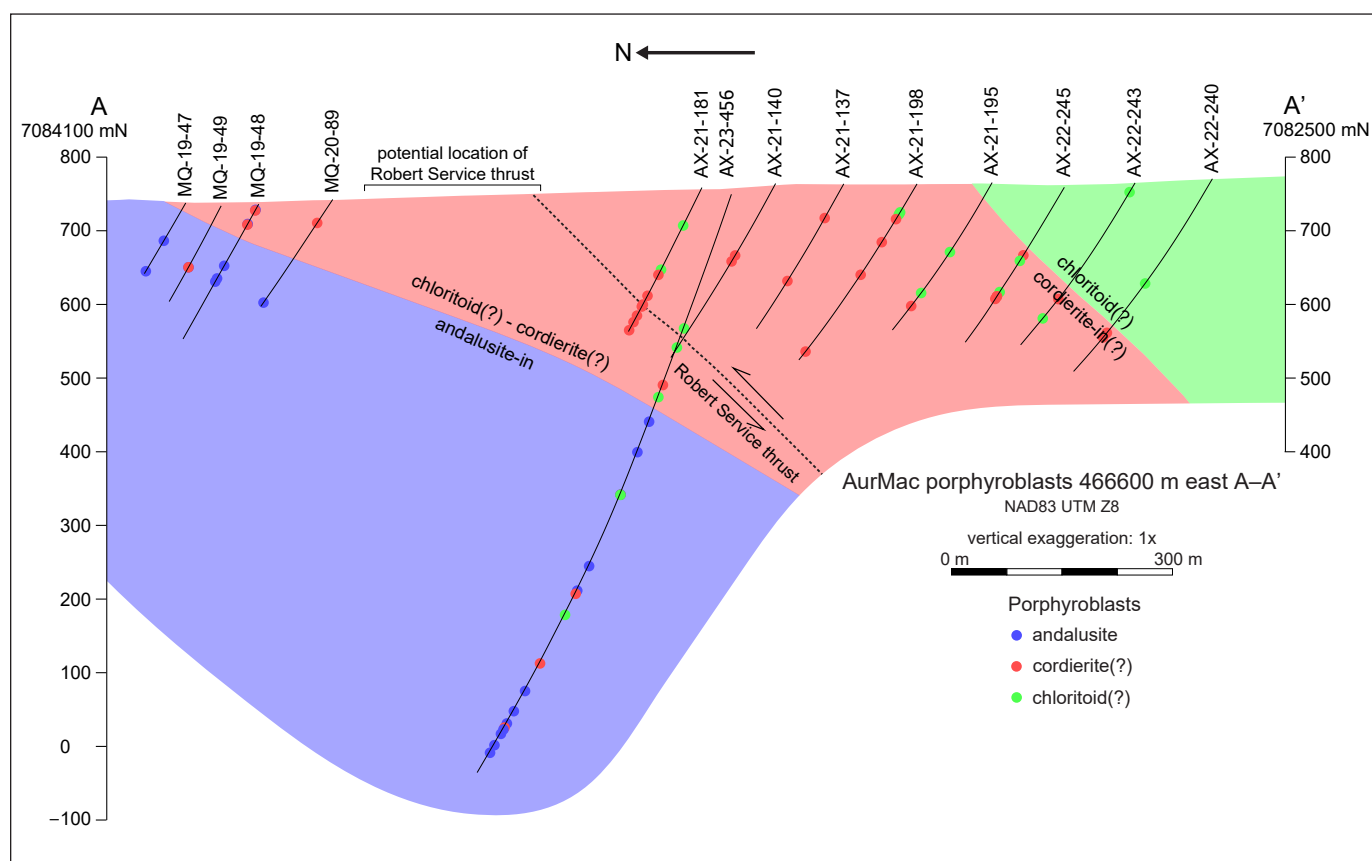


Figure 15. Cross section A-A' along 466600 mE from 7084100 mN to 7082500 mN (UTM Zone 8) illustrating observed metamorphic isograds.

Visible gold is common in vein-hosted mineralization, and is most often observed intergrown with fine-grained acicular and radiating lead-bismuth sulphosalts and less frequently in arsenopyrite aggregates. Reflected light petrography indicates that the majority of visible gold mineralization occurs as pyrrhotite–electrum–lead–bismuth sulphosalts ± chalcopyrite fracture fill in earlier sulphides and quartz (Fig. 18).

Alteration associated with vein mineralization consists of centimetre to metre-scale zones of silicification, sericitization, albitization and biotite-destructive bleaching. Due to the mineralogical variability in host rock metasedimentary rocks, distinguishing mineralization-related sericitization and silicification from metamorphic white micas in schists and more siliceous protoliths can be challenging.

Skarn

In the Airstrip deposit, and to a lesser extent in the Powerline deposit, gold mineralization occurs within pyrrhotite-bearing skarn horizons (Fig. 16b; Gray and

Thom, 2021). The skarn horizons are characterized by massive to laminated textures, featuring relict foliation and compositional banding, and are composed of calcite, quartz, clinopyroxene, amphibole, garnet and scheelite, and sulphides generally comprise <10% of the assemblage. Sulphides consist predominantly of fine-grained to blebby disseminated to net-textured pyrrhotite with minor amounts of intergrown, very fine grained chalcopyrite (Fig. 19) and <1% early, fine-grained disseminated euhedral pyrite and arsenopyrite.

Lead-zinc-silver veins and breccias

Polymetallic silver-lead-zinc mineralization on the AurMac property is rare, typically presenting as sub-centimetre-scale veinlets and breccias, and crosscuts gold-bearing sheeted veins and skarns at the AurMac property.

Gangue minerals present in veins and breccias consist of siderite, quartz and calcite. Sulphide mineralization consists of sphalerite and galena, and accessory arsenopyrite, pyrite, chalcopyrite and pyrrhotite.

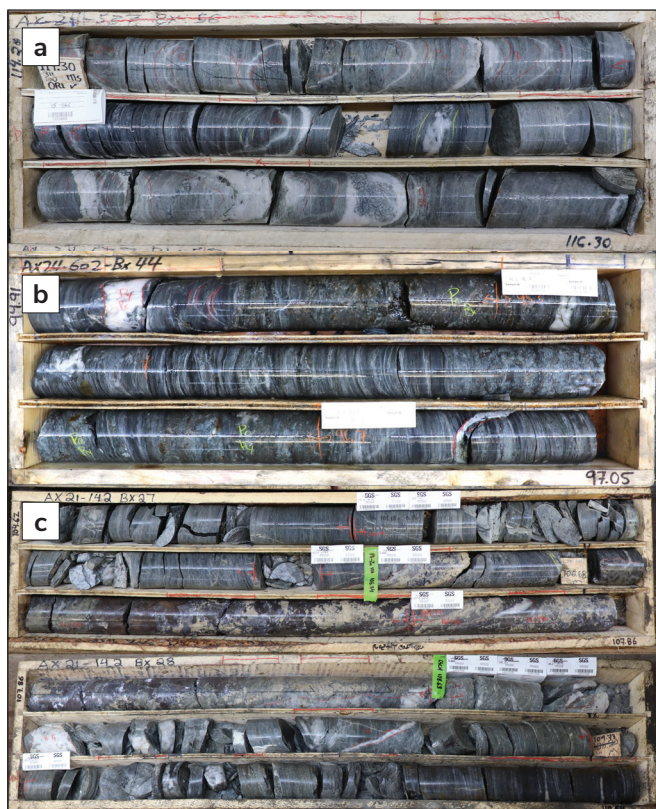


Figure 16. Core photos from drillholes on the AurMac property. Core diameter is 71 mm (HTW). **(a)** Sheeted vein gold mineralization hosted in mica-quartz schist in drillhole AX-24-537. **(b)** Skarn mineralization in drillhole AX-24-602. **(c)** Semi-massive siderite-quartz-sphalerite-galena ± pyrite-arsenopyrite-pyrrhotite vein (75 cm true width) intersected in drillhole AX-21-142.

This mineralization is believed to be analogous to that found in the Keno Hill silver district, which also hosts argentiferous tetrahedrite, native silver, and the silver-bearing sulphosalts polybasite, stephanite and pyrargyrite (Blais et al., 2024), although these minerals have yet to be identified in mineralization on the AurMac property.

In 2021, a 75 cm (true-width) semi-massive siderite-quartz-sphalerite-galena ± pyrite-arsenopyrite-pyrrhotite vein (Fig. 16c) was intersected in drillhole AX-21-142. The steeply east-southeast dipping vein strikes north with a dip and dip direction of approximately 80° toward 110°, and shares an attitude not dissimilar to vein orientations observed at the Bellekeno and Onek vein systems, Lucky Queen and Flame and Moth veins, and the Birmingham deposits of the Keno Hill silver district (Blais et al., 2024).

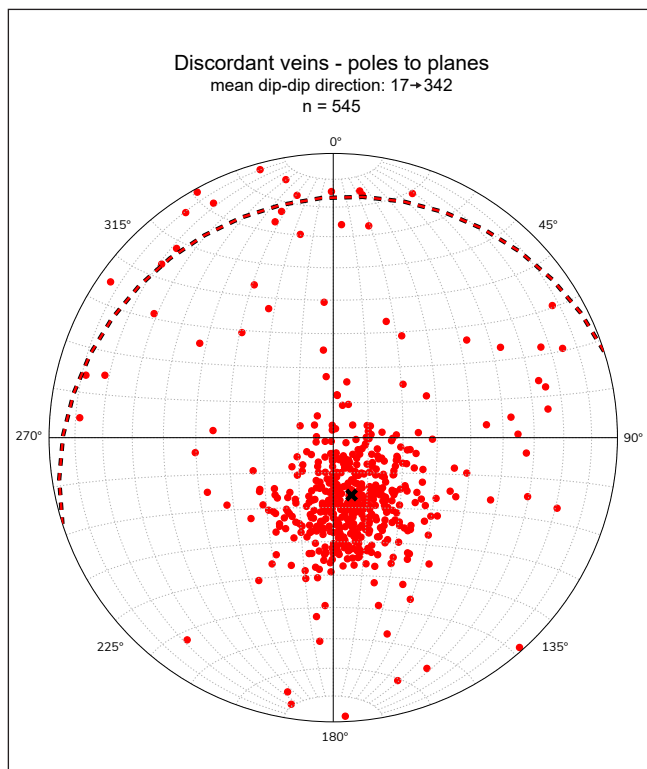


Figure 17. Stereonet depicting poles-to-planes of shallowly north-dipping gold-bearing sheeted veins.

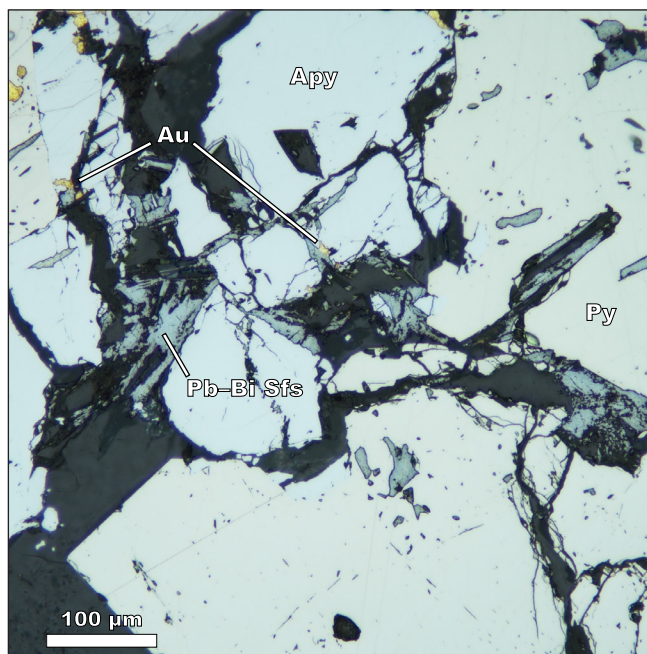


Figure 18. Reflected light photomicrograph of lead-bismuth sulphosalts (Pb-Bi Sfs) and electrum (Au) as fracture fill in arsenopyrite (Apy) and pyrite (Py).

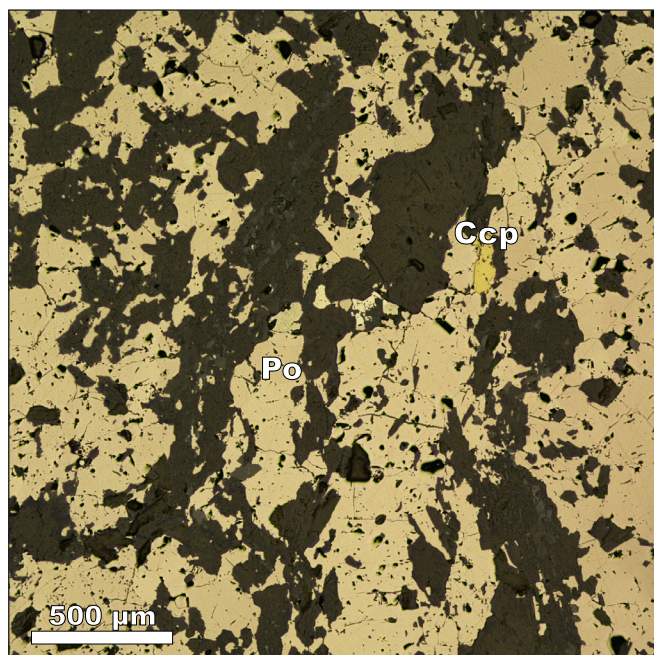


Figure 19. Reflected light photomicrograph of sulphide-bearing skarn composed of net-textured pyrrhotite (Po) and chalcopyrite (Ccp) surrounding a quartz and feldspar matrix.

Evidence for RIRGS-style mineralization

Although an underlying intrusion has yet to be identified at the AurMac deposits, gold mineralization observed on the property exhibits characteristics typical of intrusion-hosted RIRGS, similar to those at the nearby Dublin Gulch property. At the Powerline deposit, gold is hosted in sulphide-poor, centimetre-scale, sheeted quartz veins and is strongly associated with bismuth, which parallels the mineralization style at Dublin Gulch. Both deposits also share a sulphide assemblage including arsenopyrite, pyrite, pyrrhotite, pyrite, sphalerite and bismuth-bearing minerals (Harvey et al., 2023). Furthermore, a spatial relationship with skarn horizons, as seen in at the Wolf Skarn deposit proximal to the Dublin Gulch pluton, closely resembles the Airstrip deposit at the AurMac property, suggesting the potential presence of an unidentified intrusion on, or near the AurMac property (Kirk, 2016). The progressive increase in metamorphic grade observed in porphyroblasts through the outlined section, from chloritoid to cordierite and andalusite (Figs. 6, 14), also supports the presence of a potential heat source situated north of the Airstrip zone. Given these observations, and that mineralization in known RIRGS is typically hosted within the carapace and

surrounding hornfels of intrusions (Hart, 2007), the AurMac property demonstrates considerable potential for the discovery of intrusion-hosted mineralization. AurMac deposits also highlight the existence of large-scale, bulk-tonnage, sediment-hosted intrusion-related gold systems, which may occur elsewhere in the region.

References

- Abbott, G., 1997. Geology of the upper Hart River area, eastern Ogilvie Mountains, Yukon Territory (116A/10, 116 A/11). Exploration and Geological Services Division, Yukon, Indian and Northern Affairs Canada, Bulletin 9, 92 p.
- Anders, E. and Grevesse, N., 1989. Abundances of the elements: Meteoritic and solar. *Geochimica et Cosmochimica Acta*, vol. 53, no. 1, p. 197–214.
- Blais, J., Muñoz, M., Vink, C., Baoyao, T. and Blattman, M., 2024. NI 43-101 Technical Report on the Keno Hill Mine, Yukon, Canada. NI 43-101 technical report prepared by Mining Plus Canada Consulting Ltd. for Hecla Mining Company. Submitted March 28, 2024, 313 p. <https://www.sedarplus.ca/csa-party/records/document.html?id=173ac1c40d3944929606358b4a9f7372659b9c053818a9e1b651696c43af59e1> [accessed 2024/11/27].
- Colpron, M., Logan, J.M. and Mortensen, J.K., 2002. U–Pb zircon age constraint for late Neoproterozoic rifting and initiation of the lower Paleozoic passive margin of western Laurentia. *Canadian Journal of Earth Sciences*, vol. 39, no. 2, p. 133–143.
- Gabrielse, H., Murphy, D.C., Mortensen, J.K., Haggart, J.W., Enkin, R.J. and Monger, J.W.H., 2006. Cretaceous and Cenozoic dextral orogen-parallel displacements, magmatism, and paleogeography, north-central Canadian Cordillera. In: *Paleogeography of the North American Cordillera: Evidence for and against large-scale displacements*, J.W. Haggart, R.J. Enskin and J.W.H. Monger (eds.), Geological Association of Canada Special Paper 46, p. 255–276.
- Gordey, S.P. and Anderson, R.G., 1993. Evolution of the northern Cordilleran miogeocline, Nahanni map area (105I), Yukon and Northwest Territories. *Geological Survey of Canada Memoir*, no. 428, 214 p.

- Gray, P. and Thom, J., 2021. Yukon Mineral Exploration Program (YMEP) final report for a 2020 Target Evaluation Program on the AurMac Property. Yukon Mineral Exploration Program (YMEP) Report 2020-14, 305 p.
- Hart, C.J.R., 2007. Reduced intrusion-related gold systems. In: Mineral Deposits of Canada: A synthesis of major deposit types, district metallogeny, the evolution of geological provinces, and exploration methods, W.D. Goodfellow (ed.), Geological Association of Canada, Mineral Deposits Division, Special Publication No. 5, p. 95–112.
- Hart, C.J., Baker, T. and Burke, M., 2000. New exploration concepts for country-rock-hosted, intrusion-related gold systems: Tintina gold belt in Yukon. In: The Tintina gold belt: concepts, exploration and discoveries, Special Volume 2, T.L. Tucker and M.T. Smith (eds.), British Columbia and Yukon Chamber of Mines, p. 145–172.
- Hart, C.J., Mair, J.L., Goldfarb, R.J. and Groves, D.I., 2004. Source and redox controls on metallogenic variations in intrusion-related ore systems, Tombstone-Tungsten belt, Yukon Territory, Canada. *Earth and Environmental Science Transactions of The Royal Society of Edinburgh*, vol. 95, no. 1–2, p. 339–356.
- Harvey, N., Gray, P., Winterton, J., Jutras, M. and Levy, M., 2023. Technical Report, Eagle Gold Mine, Yukon Territory, Canada. NI 43-101 technical report prepared by Victoria Gold Corporation. Submitted April 10, 2023, 333 p. <https://www.sedarplus.ca/csa-party/records/document.html?id=952a15f1d0fd09d99049027e54d871659b037d1767177f2a6a6e111fed8019f6> [accessed 2024/11/27].
- Kirk, A., 2016. Paragenesis, geochemistry and metallogeny of the Dublin Gulch intrusion-related Au deposit, Yukon Territory. Unpublished MSc thesis, Memorial University, Newfoundland, Canada, 362 p.
- Mair, J.L., Hart, C.J. and Stephens, J.R., 2006. Deformation history of the northwestern Selwyn basin, Yukon, Canada: Implications for orogen evolution and mid-Cretaceous magmatism. *Geological Society of America Bulletin*, vol. 118, no. 3–4, p. 304–323.
- McOnie, A., 2016. The Keno Hill silver mining district. GAC-MAC 2016 Whitehorse Field Trip Guide Book, 69 p. and 2 maps.
- Mortensen, J.K. and Thompson, R.I., 1990. A U-Pb zircon-baddeleyite age for a differentiated mafic sill in the Ogilvie Mountains, west-central Yukon Territory. *Geological Survey of Canada Paper* 89-02, p. 23–28.
- Murphy, D.C., 1997. Geology of the McQuesten River region, northern McQuesten and Mayo map areas, Yukon Territory (115P/14, 15, 16, 105M/13, 14). Exploration and Geological Services Division, Yukon, Indian and Northern Affairs Canada, Bulletin 6, 122 p.
- O’Dea, M., Carlson, G., Harris, S., Fields, M., Tucker, T.L. and Smith, M.T., 2000. Structural and metallogenic framework for the Scheelite Dome deposit, Yukon Territory. In: The Tintina gold belt: concepts, exploration, and discoveries, Special Volume 2, T.L. Tucker and M.T. Smith (eds.), British Columbia and Yukon Chamber of Mines, Cordillera Roundup January 2000, p. 115–130.
- Pearce, J.A., 1996. A user's guide to basalt discrimination diagrams. In: Trace Element Geochemistry of Volcanic Rocks: Applications for Massive Sulphide Exploration, D.A. Wyman (ed.), Geological Association of Canada, Short Course Notes 12, p. 79–113.
- Rasmussen, K.L., 2013. The timing, composition, and petrogenesis of syn- to post-accretionary magmatism in the northern Cordilleran miogeocline, eastern Yukon and southwestern Northwest Territories. Unpublished PhD thesis, University of British Columbia, British Columbia, Canada, 788 p.
- Read, P., McOnie, A. and Iles, S., 2020. Geology of the Keno Hill district. Yukon Geological Survey, Open File 2020-42, 2 sheets, scale 1:25 000 and 1:2500.
- Roots, C.F. and Abbott, G., 1988. Cambro-Ordovician volcanic rocks in the eastern Dawson map area, Ogilvie mountains, Yukon. In: Yukon Geology Volume 2, J.G. Abbott (ed.), Exploration and Geological Services Division, Indian and Northern Affairs Canada, p. 81–87.

- Skipton, D. and Maw, L., 2021. Updated geology of the Clark Lakes area in central Yukon (parts of 106D/2, 3, 6 and 7). In: Yukon Exploration and Geology 2020, K.E. MacFarlane (ed.), Yukon Geological Survey, p. 73–94.
- Stephens, J.R., Oliver, N.H.S., Baker, T. and Hart, C.J.R., 2000. Structural evolution and controls on gold mineralization at Clear Creek, Yukon. In: Yukon Exploration and Geology 1999, D.S. Edmond and L.W. Weston (eds.), Exploration and Geological Services Division, Yukon Region, Indian and Northern Affairs Canada, p. 151–163.
- Stephens, J.R., Mair, J.L., Oliver, N.H., Hart, C.J. and Baker, T., 2004. Structural and mechanical controls on intrusion-related deposits of the Tombstone Gold Belt, Yukon, Canada, with comparisons to other vein-hosted ore-deposit types. *Journal of Structural Geology*, vol. 26, no. 6–7, p. 1025–1041.
- Sun, S.S. and McDonough, W.F., 1989. Chemical and isotopic systematics of oceanic basalts: Implications for mantle composition and processes. *Geological Society of London, Special Publications*, no. 42, p. 313–345.
- Thornton, T., Jutras, M. and Malhotra, D., 2024. Technical Report, AurMac Property, Mayo Mining District, Yukon Territory, Canada. NI 43-101 technical report prepared by JDS Energy & Mining Inc. for Banyan Gold Corporation. Submitted March 18, 2024, 327 p., <https://www.sedarplus.ca/csa-party/records/document.html?id=c2f3326a6bbde1f106d51acaacea522b6d8df8c921d6104b0f1d085c25bd0574> [accessed 2024/11/27].
- Yukon Geological Survey, 2020. A digital atlas of terranes for the northern Cordillera. Yukon Geological Survey, <https://data.geology.gov.yk.ca/Compilation/2> [accessed 2024/09/19].
- Yukon Geological Survey, 2022. Yukon Digital Bedrock Geology. Yukon Geological Survey, <https://data.geology.gov.yk.ca/Compilation/3> [accessed 2024/09/19].
- Yukon Geological Survey, 2023a. Yukon Geochronology – A database of Yukon isotopic age determinations. Yukon Geological Survey, <https://data.geology.gov.yk.ca/Compilation/22> [accessed 2024/09/19].
- Yukon Geological Survey, 2023b. Yukon Litho geochemistry data set. Yukon Geological Survey, <https://data.geology.gov.yk.ca/Compilation/35> [accessed 2024/09/19].